

# Eigenvalues for Waveguides Containing Re-Entrant Corners by a Finite-Element Method with Superelements

Bernard Schiff and Zohar Yosibash

**Abstract**—Superelements have been developed to enable the finite-element method to be used for computing accurate eigenvalues of the Laplacian over domains containing re-entrant corners of arbitrary angle. A truncated asymptotic expansion of the solution is employed in the region of the corner, and linear blending is used over the remainder of the superelement to provide a smooth transition to piecewise quadratics over the superelement boundary. The superelement thus conforms with the usual triangular or quadrilateral isoparametric elements used over the remainder of the domain, and can be easily incorporated into a general finite-element program. The scheme has been tested on various waveguides containing one or more angles of size  $3\pi/2$  or  $2\pi$ , and also on domains containing various other angles, and the results agree well with those obtained by other methods, mostly of less general applicability.

**Index Terms**—Finite-element methods, singularities, Helmholtz equation, eigenvalues.

## I. INTRODUCTION

**R**IDGED AND other waveguides whose cross sections contain one or more re-entrant corners, often of angle  $3\pi/2$  or  $2\pi$ , are frequently used in microwave devices and circuits. It is, therefore, important to be able to obtain accurate values for the cutoff frequencies of the first few modes of propagation in waveguides of this type. A variety of methods have been used for this purpose, and some of the more accurate methods are described in [1]–[6]. The flexibility of the finite-element method would seem to make it ideally suited for this purpose. The standard finite-element schemes, however, yield comparatively poor results when applied to problems containing a re-entrant corner, due to the singular nature of the solution there. One method used to circumvent this difficulty is to refine the mesh locally in the neighborhood of such a corner [7]. Another approach utilizes the known asymptotic expansion for the solution in the neighborhood of the singularity, for example, by suitably modifying the shape functions over each of the elements possessing a node at the corner [8], [9] or by augmenting the trial function basis by the addition of functions possessing a suitable singular behavior there [10], [11]. In an earlier paper [12], Schiff outlined a method that used a combination of these two approaches. The

basic idea was to cover the region of each re-entrant corner with a “singular superelement,” whose stiffness matrix could be calculated once and for all for a given geometry. The superelement was constructed so as to be conformal with linear triangular or bilinear rectangular elements, which were then employed over the remainder of the domain. The method was applied to determine cutoff frequencies for TE and TM modes in guides containing one or more re-entrant corners of angle  $3\pi/2$  or  $2\pi$ . This paper embodies a wide generalization of these ideas. Firstly, the superelements have been designed to conform with six- (triangular) or eight-node (quadrilateral) isoparametric quadratic elements over the rest of the domain, enabling much higher accuracy to be achieved at a moderate cost. Secondly, the re-entrant angles are not restricted to be of magnitude  $3\pi/2$  or  $2\pi$ , so that the method can be applied to more complicated geometries. Finally, the trial function over the superelement has been chosen in a different way, so as to provide a better approximation to the true solution in the region of the corner. The present method is described in Section II. The results obtained for various test cases are described in Section III, and the conclusions are summarized in Section IV.

## II. THE COMPUTATIONAL SCHEME

The TE and TM fields for the waveguide may be derived from potentials that satisfy the Helmholtz equation

$$\nabla^2 \Psi(x, y, z) + k_0^2 \Psi(x, y, z) = 0 \quad (1)$$

where  $k_0$  is the propagation constant in free space. Taking the guide axis to be in the  $z$ -direction, we assume that  $\Psi(x, y, z) = \psi(x, y) \exp^{i\beta z}$  and, hence, obtain the equation

$$\nabla_T^2 \psi(x, y) + k_T^2 \psi(x, y) = 0 \quad (2)$$

where  $k_T^2 = k_0^2 - \beta^2$  and  $\nabla_T^2$  denotes the two-dimensional Laplacian. Thus, we wish to solve

$$(\nabla_T^2 + \lambda) \psi(x, y) = 0, \quad \text{in } \Omega \quad (3)$$

with boundary conditions

$$\psi = 0, \quad \text{on } \partial\Omega \quad (\text{TM modes})$$

or

$$\frac{\partial \psi}{\partial n} = 0, \quad \text{on } \partial\Omega \quad (\text{TE modes}) \quad (4)$$

where the eigenvalue is  $\lambda = k_T^2$ .

Manuscript received January 28, 1998.

B. Schiff, deceased, was with the School of Mathematical Sciences, Raymond and Beverly Sackler Faculty of Exact Sciences, Tel Aviv University, Tel Aviv 69978, Israel.

Z. Yosibash is with the Pearlstone Center for Aeronautical Engineering Studies, Department of Mechanical Engineering, Ben-Gurion University of the Negev, Beer-Sheva 84105, Israel (e-mail: zohary@pversion.bgu.ac.il).

Publisher Item Identifier S 0018-9480(00)00852-8.

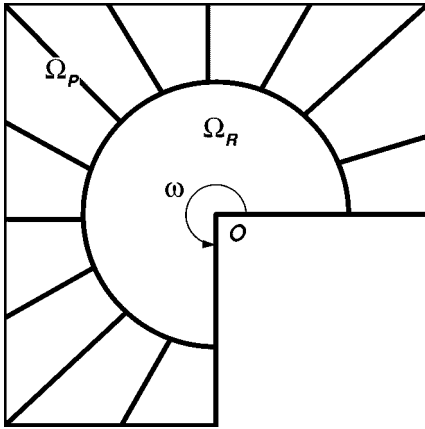


Fig. 1. Typical superelement ( $\omega = 3\pi/2$ ).

To solve the problem by the finite-element method, we use a superelement over the immediate neighborhood of each re-entrant corner and cover the remainder of  $\Omega$  with the usual six-node triangular or eight-node quadrilateral quadratic isoparametric elements. The superelement used in the previous method [12] was composed of two regions. The inner region was divided uniformly into rectangular elements, the trial function over each such element being taken as the bilinear interpolant to the asymptotic expansion, suitably truncated, for the solution in the neighborhood of the corner. Over the second region, the transition region, a piecewise bilinear trial function was used to match up between the elements on the edge of the inner region and the linear or bilinear elements adjoining the superelement.

In the present method, the superelement is again divided into an inner and a transition region. The geometry of a typical superelement is illustrated in Fig. 1. The inner region  $\Omega_R$  is taken to be a sector of a circle centered at the corner, and the trial function over this region is taken to be the asymptotic expansion for the solution of the problem in the vicinity of the corner (instead of an interpolant to this series in the previous method). Let us take polar coordinate with origin at the re-entrant corner  $\bigcirc$ . If the boundaries of the re-entrant corner are at  $\theta = 0$  and  $\theta = \omega$ , then the asymptotic expansions are

$$\psi(r, \theta) = \sum_{j=1}^{\infty} \sum_{\ell=0}^{\infty} c_{j\ell} r^{j\gamma+2\ell} \sin(j\gamma\theta) \quad (\text{TM}) \quad (5)$$

$$\psi(r, \theta) = \sum_{j=0}^{\infty} \sum_{\ell=0}^{\infty} c_{j\ell} r^{j\gamma+2\ell} \cos(j\gamma\theta) \quad (\text{TE}) \quad (6)$$

where  $\gamma = \pi/\omega$ . We use a truncated form of this series containing all of the terms for which  $j\gamma + 2\ell \leq M$  for a suitable value of  $M$ .

The transition region  $\Omega_P$  is covered by a single ring of elements, each of which has two edges that are straight lines in radial directions, a third edge being a straight line constituting part of the boundary of the superelement. The fourth edge lies on a portion of the circular boundary of the inner region  $\Omega_R$ . The trial function over each element of the transition region behaves as a quadratic (determined by the nodal values at the two

ends and the midpoint) over each straight edge, and takes on the value of the sum of the truncated series along the curved side. The function inside the element is obtained by quadratic blending between the values along the four edges of the element. This superelement was originally designed to be used when solving Laplace's equation over regions containing re-entrant corners, and full mathematical details of the construction of the trial functions and the computation of the superelement stiffness matrix are given in [13] by the authors on this topic. The computation of the massmatrix needed for this paper is performed in a similar manner. We will, therefore, here only outline the salient ideas. The integration over the inner region was performed using tensor product  $8 \times 8$  Gaussian integration. For each element of the transition region  $\Omega_P$ , a quadratic isoparametric transformation was first used to transform the element into a square, and the integration was then performed in the standard plane using  $8 \times 8$  Gaussian quadrature. The superelement conforms with the usual quadratic elements outside. Thus, the trial functions would satisfy the conforming condition exactly over the whole domain were it not for the "variational crimes" ([14, Ch. 4]) committed in the use of numerical quadrature formulas and the inaccuracies inherent in the use of the six- or eight-point isoparametric quadratic transformation used to map each element onto the standard element.

A small library of stiffness and mass matrices for different geometric configurations has been prepared. When solving a particular problem, the contributions from the superelement to the global stiffness and mass matrices are added at the assembly stage in the same manner as for the usual types of element. The superelements may thus be incorporated into a general finite-element program with no difficulty.

### III. NUMERICAL RESULTS

We have tested the method on a variety of cases for which accurate values for the cutoff frequencies of the first few modes have been obtained by other methods. We now describe the various cases treated. In each case, we list the results for two finite-element meshes with differing numbers of degrees of freedom (d.o.f.) in order to indicate the degree of convergence achieved. Unless otherwise stated, we list the value of the cutoff wavenumber, which we denote as usual by  $k_c$ , in radians per unit length, for each mode. The corresponding eigenvalue for (3) is, therefore,  $\lambda = k_c^2$ .

#### A. L-Shaped Guide

The domain is illustrated in Fig. 2. For the TM modes, highly accurate results have been obtained by Fox *et al.* [15] and for some of the modes also by Fix *et al.* [10]. Fox *et al.* use the method of "special solutions," expanding the solution in terms of a series of solutions of the Helmholtz equation and determining the eigenvalues by requiring the (truncated) series to satisfy the boundary conditions at a number of equally spaced points on the boundary. They obtained convergence to four digits after the decimal point with only eight terms in the series (they were able to obtain such a high accuracy so economically by utilizing the symmetry properties of this particular domain). Fix *et al.* used finite elements with a basis of

TABLE I  
VALUES OF  $k_c$  FOR AN L-SHAPED GUIDE

| Ref.       | TM Modes |        |        |        |        | TE Modes |        |        |        |        |
|------------|----------|--------|--------|--------|--------|----------|--------|--------|--------|--------|
| [15], [10] | 3.1048   | 3.8984 | 4.4429 | 5.4334 | 5.6491 | 1.2135   | 1.8796 | 3.1402 | 3.1402 | 3.3736 |
| [6]        | 3.1083   | 3.8957 | 4.4400 | 5.4266 | 5.6477 | 1.2012   | 1.8516 | 3.0959 |        | 3.3314 |
| [3]        | 3.0910   | 3.8964 | 4.4392 | 5.4308 |        |          |        |        |        |        |
| Present:   |          |        |        |        |        |          |        |        |        |        |
| 107 d.o.f. | 3.1069   | 3.9023 | 4.4492 | 5.4540 | 5.6742 | 1.2150   | 1.8801 | 3.1444 | 3.1444 | 3.3776 |
| 192 d.o.f. | 3.1054   | 3.8989 | 4.4438 | 5.4375 | 5.6551 | 1.2149   | 1.8800 | 3.1423 | 3.1423 | 3.3757 |

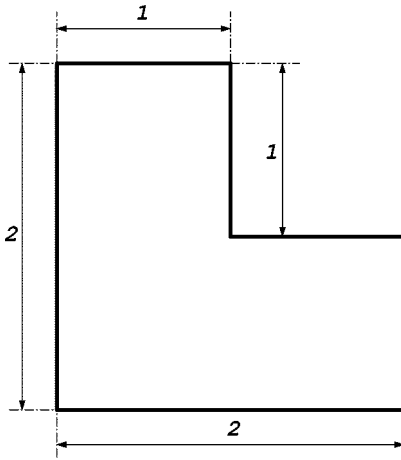


Fig. 2. L-shaped domain.

bicubic splines augmented by the first few terms of the asymptotic expansion multiplied by a suitable factor to satisfy the boundary conditions. Their results agreed with those of [15] to at least six significant digits. Guan and Su [6] and Swaminathan *et al.* [3] obtained values for the first four TM and the first four TE modes. The former used finite differences over a uniform mesh, employing approximately 2500 d.o.f., while the latter used an equivalent-surface integral equation, which they solved by the method of moments with piecewise linear functions, obtaining the eigenvalues by an iterative technique. The current method was applied using an L-shaped superelement around the singularity. In Table I, we compare our values of  $k_c$  with those of previous calculations. The agreement with the results of [10] and [15] is especially good.

### B. Quadruple-Ridged Guide

The domain is shown in Fig. 3, and represents one-half of the guide cross section, the other half being obtained by reflection in the  $y$ -axis. There are four re-entrant corners, and thus we employ four L-shaped superelements. Computations for this guide have also been made by Dasgupta and Saha [2], using a method developed by Montgomery [1], Gil and Zapata [9], and Webb [11]. Montgomery's method will be described in Section III-C. Gil and Zapata use six-node quadratic finite elements and, over the triangles having a node at a singularity, they use a geometric transformation to give the trial function the same behavior in the radial direction as the leading term of the asymptotic expansion for the solution. Webb used quadratic finite elements supplemented by singular trial functions for the electric field, introducing a penalty term into the variational formulation to remove spurious modes. The results of the various calculations are listed

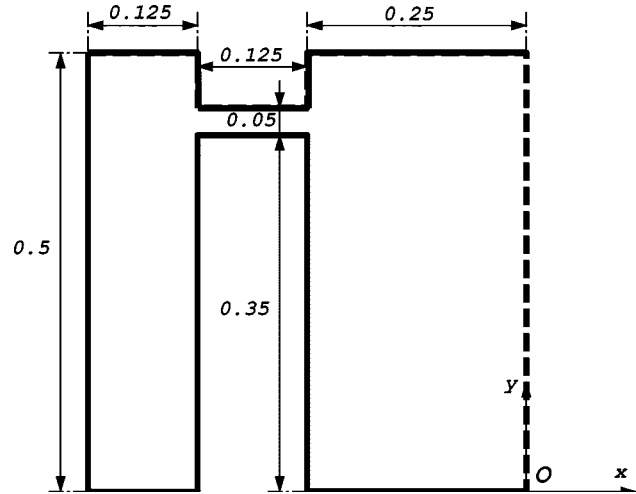


Fig. 3. Domain for quadruple-ridged guide.

TABLE II  
VALUES OF  $k_c$  FOR TE MODES IN THE "QUADRUPLE-RIDGED" GUIDE

| Ref.       | $k_c$ |       |
|------------|-------|-------|
| [2]        | 1.822 | 2.322 |
| [9]        | 1.814 | 2.312 |
| [11]       | 1.808 | 2.300 |
| Present:   |       |       |
| 151 d.o.f. | 1.814 | 2.311 |
| 295 d.o.f. | 1.808 | 2.304 |

in Table II. The excellent agreement between the results of the current scheme with the finer mesh and those of Webb should be noted. The results for the coarser scheme are very close to those of Gil and Zapata, giving an indication of the degree of convergence.

### C. Symmetric Double-Ridge Guide

This guide has been treated by a variety of methods. The problem is to be solved over a domain consisting of a quarter of the guide cross section, as shown in Fig. 4. The remainder of the guide is obtained by reflecting this domain about the  $x$ - and/or  $y$ -axis. Montgomery treated this guide in detail in [1]. He developed the solution inside each rectangle of which the domain is composed in a "modal expansion," the modes being those for a rectangular guide possessing the given cross section. The coefficients in the expansions and the values of  $k_c$  were determined by solving an integral equation for the normal component of the electric field over the interface between the two regions. Israel and Miniowitz [7] solved this problem using quintic Hermite finite elements with local mesh refinement in

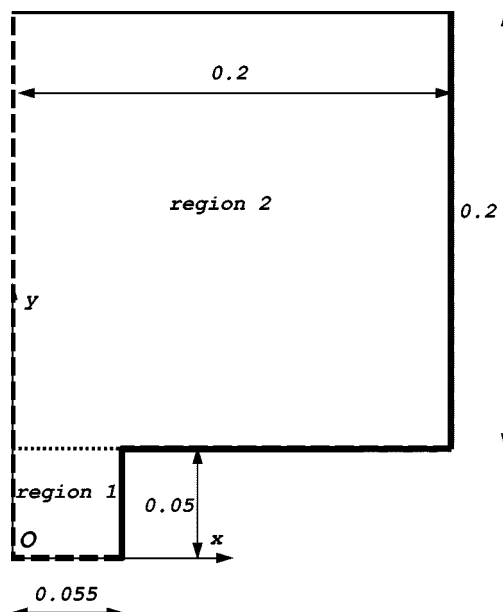


Fig. 4. Domain for symmetric double-ridge guide.

the neighborhood of the singularity, while Guan and Su [6] and Gil and Zapata [9] employed their methods as described in Sections III-A and III-B, respectively. We solved the problem using an L-shaped element over the neighborhood of the singularity at the point  $x = 0.055$ ,  $y = 0.05$ . The values of  $k_c$  for the first few TE modes are listed and compared with the previous results in Table III. It will be seen that for some of the modes, we obtained pairs of values lying very close to one another. In each case, the two eigenfunctions corresponding to the pair of almost identical eigenvalues were completely different from one another, indicating the presence of an almost degenerate eigenvalue. This phenomenon was reported and explained by Montgomery in [1, Sec. V] as follows: “Note the existence of so-called hybrid and trough modes. Hybrid modes are considered to be basic ridged waveguide modes of propagation. Trough modes are so named because they are rectangular waveguide type modes which exist in the trough region (region 2). . . . One should also note that the trough modes are almost degenerate for a narrow gap in respect that the TE magnetic and electric eigenvalues are almost the same.” Returning to our results in Table III, the trough modes are those for which we obtain a pair of almost equal values of  $k_c$ , and these are exactly those modes classified as such by Montgomery, as shown in diagrammatic form in [1, Fig. 3]. In Table III, we label each eigenvalue with its symmetry type, the two letters referring to s(ymmetry) or a(symmetry) of the eigenfunction with respect to reflection in the  $x$ - or  $y$ -axes, respectively. It will be noted that the two members of a pair have identical symmetry with respect to the  $y$ -axis, but opposite symmetry with respect to the  $x$ -axis. For a trough mode, being similar to a mode for the rectangular region 2, it is not surprising to find that the corresponding eigenfunction is comparatively small in region 1. Thus, the contribution from this region to the energy integral is small and there is, therefore, only a small difference between the eigenvalues for the two possible types of boundary conditions over the edge  $0 < x < 0.055$ ,  $y = 0$ . It will be seen that the

current results agree very closely with those of Israel and Minowitz [7] and Gil and Zapata [9]. There is also good agreement with the values obtained by Montgomery [1] and Guan and Su [6].

#### D. Symmetric Rectangular Coaxial Guide

The domain is illustrated in Fig. 5, and represents one-half of the guide cross section, the other half being obtained by reflection in the  $x$ -axis. The dimensions in this figure are given in meters. The guide has a slit along the line  $x = 3$ ,  $-2.5 < y < 2.5$ . Particularly accurate calculations have been made for TE modes in this guide. Guan and Su [6] used finite differences over a uniform mesh, employing approximately 15 000 d.o.f. De Leo *et al.* [4] used modal expansions over the two rectangles  $0 < x < 3$  and  $3 < x < 6$ . They take into account the singular nature of the field at the tip of the slit (the point  $x = 3$ ,  $y = 2.5$ ) by including a suitable multiplicative factor in the expression for the component of the electric field along the “interface”  $x = 3$ ,  $2.5 < y < 3$  between these two rectangles.

We have solved the problem using a square superelement around the singularity at the end of the slit. The values obtained are compared with those of previous calculations in Table IV.

The results listed in Table IV are the cutoff frequencies in megahertz instead of the wavenumbers, in order to compare easily with the results of other authors. There are additional modes not listed in this table, as we have only listed those modes for which both Guan and Su and De Leo *et al.* give results. Our results using the finer mesh agree with those of De Leo *et al.* to within 0.03% for the first two modes listed, while Guan and Su's value for the first mode differs from ours by 0.5%. This is probably due to the fact that Guan and Su's method makes no provision for the existence of the singularity.

#### E. T-Septate Guide

The domain is illustrated in Fig. 6, and represents one-half of the guide cross section, the other half being obtained by reflecting this domain in the  $x$ -axis. The guide has slits along the lines  $x = 0.25$ ,  $-0.125 < y < 0.125$  and  $0 < x < 0.25$ , and  $y = 0$ , and the modes are either symmetric or antisymmetric across the line  $0.25 < x < 1.0$ ,  $y = 0$ . Calculations for this guide have been made by Swaminathan *et al.* [3], using the method described in Section III-A, and by Shu *et al.* [5] by a somewhat similar method, except that they use a different integral equation and employ piecewise constant functions over each segment in the method of moments.

We have solved the problem using a square-shaped superelement around the singularity at the point  $x = 0.25$ ,  $y = 0.125$ . The values obtained are compared with those from previous calculations in Table V. Shu *et al.* were apparently unable to resolve the difference between the two lowest TE modes. Our results altogether agree more closely with those of Swaminathan *et al.* The agreement with the results of these authors for the TE modes is, however, less satisfactory than for the other guides listed in the previous sections. This may be due to the fact that they had to modify their method for this case, as is mentioned in their paper.

TABLE III  
VALUES OF  $k_c$  FOR TE MODES IN THE SYMMETRIC DOUBLE-RIDGE GUIDE

| Ref.           | $k_c$ 's |         |         |         |         |         |         |         |         |
|----------------|----------|---------|---------|---------|---------|---------|---------|---------|---------|
| [1]            | 0.14371  | 0.31656 |         | 0.52098 | 0.61902 | 0.67117 | 0.69732 |         |         |
| [7] (164 dof.) | 0.14397  |         |         |         | 0.61922 | 0.6713  |         |         |         |
| [9]            |          |         |         |         |         |         |         |         |         |
| 54 d.o.f.      | 0.1439   |         |         |         | 0.6203  | 0.6731  |         |         |         |
| 141 d.o.f.     | 0.1439   |         |         |         | 0.6193  | 0.6714  |         |         |         |
| [6]            | 0.1434   | 0.3168  |         |         | 0.6192  | 0.6705  | 0.6975  |         |         |
| Present:       |          |         |         |         |         |         |         |         |         |
| Sym. Type      | a s      | s a     | a a     | s s     | a s     | s s     | a s     | s a     | a a     |
| 72 d.o.f.      | 0.14390  | 0.31578 | 0.31707 | 0.52215 | 0.61977 | 0.61978 | 0.67232 | 0.69757 | 0.69858 |
| 122 d.o.f.     | 0.14385  | 0.31572 | 0.31673 | 0.52159 | 0.61931 | 0.61931 | 0.67137 | 0.69647 | 0.69775 |

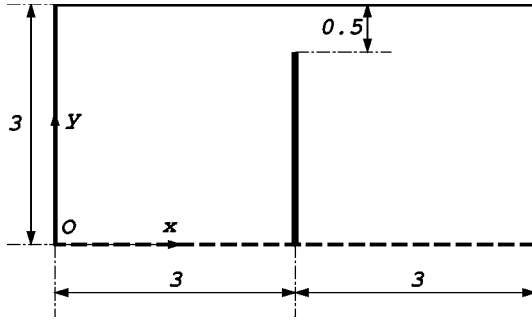


Fig. 5. Domain for symmetric rectangular coaxial guide.

TABLE IV  
CUTOFF FREQUENCIES IN MEGAHERTZ FOR TE MODES IN SYMMETRIC RECTANGULAR COAXIAL GUIDE

| Ref.       | Cutoff Frequencies |        |        |        |        |        |
|------------|--------------------|--------|--------|--------|--------|--------|
| [6]        | 14.203             | 31.786 | 57.351 | 64.032 | 79.399 | 94.605 |
| [4]        | 14.270             | 31.819 | 57.374 | 64.089 | 79.451 | 94.558 |
| Present:   |                    |        |        |        |        |        |
| 94 d.o.f.  | 14.331             | 31.867 | 57.551 | 64.413 | 80.057 | 95.684 |
| 156 d.o.f. | 14.274             | 31.822 | 57.409 | 64.140 | 79.565 | 94.835 |

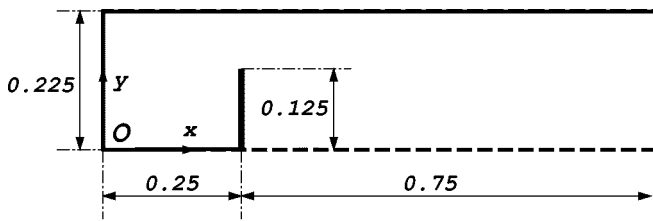


Fig. 6. Domain for T-septate guide.

#### F. Accuracy of the Method

The values obtained using the finer mesh agree with the nearest results obtained by other methods to within a maximum difference of 0.3%, in most cases the difference being no more than 0.12%. For the coarse mesh, the maximum difference with the nearest other calculations was 1.5% and, in most cases, the difference was less than 0.5%. The only exception was for the TE modes of the T-septate guide, where the current values differed from the nearest values (those of Swaminathan *et al.*) by as much as 2.7% for both meshes. We assume that this is due to the difficulty encountered by these authors for this particular guide.

In order to further verify the accuracy of the method, calculations were also performed for the above-mentioned guides with an HP-version finite-element scheme, using varying numbers of d.o.f. The HP scheme required roughly double the number of d.o.f. used by the current method for a given accuracy. Further details will be given in [16].

#### G. Effect of the Superelement

In order to assess the degree of improvement resulting from the inclusion of the superelements, some of the computations were repeated with the superelement replaced by a number of eight-node quadratic elements similar to those that were adjacent to the superelement in the original mesh. As a typical example of the results obtained, we list in Table VI the percentage errors in the frequency for the symmetric rectangular coaxial guide discussed in Section III-D using the fine mesh with and without the superelement. The figures listed illustrate the general feature that the percentage improvement is largest for the smallest eigenvalue and decreases as the eigenvalue increases.

As regards the sensitivity of the results to the detailed construction of the superelement, it was found that the eigenvalues were very insensitive to the value of  $R_{\text{norm}}$ , the ratio of the radius  $R$  of the inner region  $\Omega_R$  to that of the largest circle that may be inscribed in the superelement. For example, in the case of the symmetric rectangular coaxial guide, the eigenvalues varied by less than 0.01% as  $R_{\text{norm}}$  varied over the range 0.9 to 0.6, and by less than 0.1% over the range from 0.9 to 0.15. The present computations were performed with  $R_{\text{norm}}$  equal to 0.9 or 0.75. The number of elements into which the region  $\Omega_P$  of the superelement is divided is equal to the number of elements of the outer region that are adjacent to the superelement. Thus, increasing the number of elements in  $\Omega_P$  will require a finer mesh in the neighborhood of the superelement. Therefore, for high accuracy, we used smaller elements near the superelement, while allowing larger elements further away, and divided the region  $\Omega_P$  accordingly. For the results quoted in Tables I–V, we divided  $\Omega_P$  into 20, 8, 12, 10 and 16 elements, respectively, for the coarse meshes, and into 24, 12, 12, 16 and 16 elements, respectively, for the fine meshes. This point will be discussed more fully in [16].

#### H. A General Re-Entrant Angle

In order to confirm that the current method is valid for a re-entrant corner of any size between  $\pi$  and  $2\pi$ , the method has also

TABLE V  
VALUES OF  $k_c$  FOR THE T-SEPTATE GUIDE

| Ref.       | TM Modes |         |         |         | TE Modes |        |        |        |
|------------|----------|---------|---------|---------|----------|--------|--------|--------|
| [3]        | 8.1293   | 10.8659 | 14.3161 | 14.5550 | 2.9752   | 3.1677 | 5.5635 | 7.2357 |
| [5]        | 8.1302   | 10.8720 | 14.3124 | 14.5439 | 3.0015   | 5.4265 | 7.2252 |        |
| Present:   |          |         |         |         |          |        |        |        |
| 116 d.o.f. | 8.1387   | 10.9209 | 14.5288 | 14.6157 | 2.9365   | 3.0847 | 5.5908 | 7.2371 |
| 202 d.o.f. | 8.1357   | 10.8886 | 14.3558 | 14.5712 | 2.9356   | 3.0824 | 5.5824 | 7.2354 |

TABLE VI  
PERCENTAGE ERRORS IN CUTOFF FREQUENCIES FOR SYMMETRIC RECTANGULAR COAXIAL GUIDE WITH AND WITHOUT THE USE OF A SUPERELEMENT FOR MODES LISTED IN TABLE IV

| With<br>Superelement (156 d.o.f.)    | 0.03 | 0.01 | 0.06 | 0.08 | 0.14 | 0.29 |
|--------------------------------------|------|------|------|------|------|------|
| Without<br>Superelement (121 d.o.f.) | 2.40 | 0.77 | 0.52 | 0.76 | 0.73 | 0.36 |

TABLE VII  
VALUES FOR CUTOFF WAVELENGTHS IN (MILLIMETERS) IN A GUIDE WITH A TRAPEZOIDAL RIDGE

| Ref.                | TE Modes |        |        |        | TM Mode |
|---------------------|----------|--------|--------|--------|---------|
| [17] : Experimental | 248.0    | 128.2  | 126.7  | 101.0  | 79.0    |
| [17] : Theoretical  | 248.4    | 127.5  | 125.4  | 98.0   | 82.5    |
| Present:            |          |        |        |        |         |
| 80 d.o.f.           | 257.53   | 129.14 | 126.89 | 100.89 | 80.20   |
| 158 d.o.f.          | 257.54   | 129.15 | 126.90 | 100.91 | 80.23   |

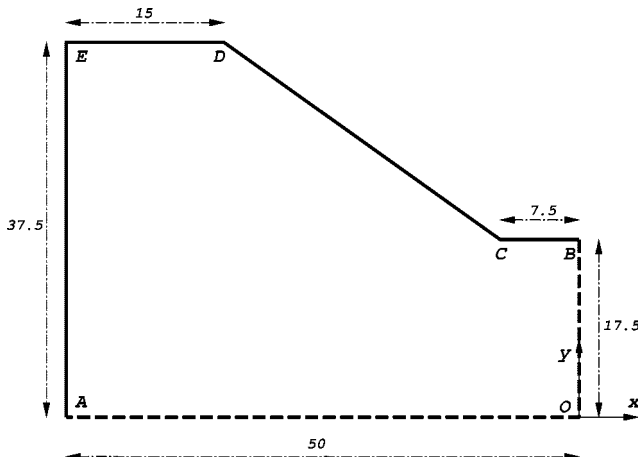


Fig. 7. Domain for trapezoidal waveguide.

been tested on the waveguide with trapezoidal ridges considered by Meinke *et al.* [17]. Meinke *et al.* use a conformal transformation to map the domain onto a rectangle, obtaining the mapping function in the form of an infinite series. Our computation is carried out on the quarter of the guide cross section shown in Fig. 7. The remainder of the guide can be obtained by reflection in the  $x$ - and/or  $y$ -axes. For the TE modes, the boundary conditions are that  $\partial u/\partial n = 0$  over the edges  $BC$ ,  $CD$ ,  $DE$ , and  $EA$  and  $u = 0$  or  $\partial u/\partial n = 0$  over  $AO$  and  $OB$  (thus, there are four different types of modes). The conditions for the TM modes are obtained from those for the TE modes by simply interchanging  $u$  and  $\partial u/\partial n$ .

Again, we treated this case with a coarser and a finer mesh, using 80 and 158 d.o.f., respectively, including the d.o.f. belonging to the superelement around the re-entrant corner at the point  $C$ . For the superelements, we used  $R_{\text{norm}} = 0.9$ , and divided them into ten and 18 elements, respectively. Meinke *et al.* give the results of their calculations and also experimental values for the first four TE modes and the lowest TM mode. The results are compared with those obtained by the current method in Table VII, in which the wavelengths are listed following [17]. It will be seen that the current results agree with the experimental values to within 0.2% in two cases, and within

1% for two more. On the other hand, the results for the lowest TE mode differ by 3.8%. The agreement with the Meinke *et al.* computational results is less favorable. We have no explanation for the size of the discrepancies, especially in view of the fact that the current results agree very well with those obtained by the HP version of the finite-element scheme mentioned in Section III-F.

The generality of the method has also been tested by determining the first three acoustic eigenfrequencies for a simplified model of an automobile interior containing re-entrant angles of sizes  $25\pi/18$  and  $29\pi/18$ , and satisfactory agreement was obtained with the experimental values and with the results of other calculations. Details of these calculations will be described in [16].

#### IV. CONCLUSION

A superelement has been designed to overcome the loss of accuracy encountered when applying the standard finite-element schemes to obtain cutoff wave numbers for TE and TM modes in waveguides whose cross sections contain corners with re-entrant angles. The results of test calculations are listed for several waveguides whose cross sections contain one or more re-entrant angles, using two different mesh sizes in each case. Our results, obtained using a moderate number of d.o.f., compare well with the most accurate values obtained by a variety of other methods. The method has also been tested successfully on domains containing various other angles to verify its suitability for re-entrant angles of any size. The superelement is compatible with six- and eight-point quadratic isoparametric elements, and can be easily incorporated in standard finite-element programs. More general methods, such as the use of edge elements, have recently been developed for solving problems in electromagnetics in which it is necessary to work with the field components directly rather than with just a scalar potential (see, e.g., reference ([18, Ch. 9]) for details). Such methods can be adapted to take account of singularities, e.g., as in Pantic-Tanner *et al.* [19] and Gil and Webb [20]. We feel, however, that for the problem addressed in this paper, the method presented has the advantage that it

achieves high accuracy while requiring only a standard finite-element program into which superelements can be incorporated.

#### ACKNOWLEDGMENT

The authors are grateful to the reviewers for useful comments.

#### REFERENCES

- [1] J. P. Montgomery, "On the complete eigenvalue solution of ridged waveguide," *IEEE Trans. Microwave Theory Tech.*, vol. MTT-19, pp. 547–555, June 1971.
- [2] D. Dasgupta and P. Saha, "Rectangular waveguide with two double ridges," *IEEE Trans. Microwave Theory Tech.*, vol. MTT-31, pp. 938–941, Nov. 1983.
- [3] M. Swaminathan, E. Arvas, T. K. Sarkar, and A. R. Djordjevic, "Computation of cutoff wavenumbers off TE and TM modes in waveguides of arbitrary cross sections using a surface integral formulation," *IEEE Trans. Microwave Theory Tech.*, vol. 38, pp. 154–159, Feb. 1990.
- [4] R. De Leo, T. Rozzi, C. Svara, and L. Zapelli, "Rigorous analysis of the GTEM cell," *IEEE Trans. Microwave Theory Tech.*, vol. 39, pp. 488–500, Mar. 1991.
- [5] S. Shu, P. M. Goggans, and A. A. Kishk, "Computation of cutoff wavenumbers for partially filled waveguides of arbitrary cross section using surface integral formulations and the method of moments," *IEEE Trans. Microwave Theory Tech.*, vol. 41, pp. 1111–1118, June 1993.
- [6] J.-M. Guan and C.-C. Su, "Analysis of metallic waveguides with rectangular boundaries by using the finite-difference method and the simultaneous iteration with the Chebyshev acceleration," *IEEE Trans. Microwave Theory Tech.*, vol. 43, pp. 374–381, Feb. 1995.
- [7] M. Israel and R. Miniowitz, "An efficient finite-element method for non-convex waveguides based on Hermitian polynomials," *IEEE Trans. Microwave Theory Tech.*, vol. MTT-35, pp. 1019–1026, Nov. 1987.
- [8] Z. Pantic and R. Mittra, "Quasi-TEM analysis of microwave transmission lines by the finite-element method," *IEEE Trans. Microwave Theory Tech.*, vol. MTT-34, pp. 1096–1103, Nov. 1986.
- [9] J. M. Gil and J. Zapata, "Efficient singular element for finite-element analysis of quasi-TEM transmission lines and waveguides with sharp metal edges," *IEEE Trans. Microwave Theory Tech.*, vol. 42, pp. 92–98, Jan. 1994.
- [10] G. J. Fix, S. Gulati, and G. I. Wakoff, "On the use of singular functions with finite-element approximations," *J. Comput. Phys.*, vol. 13, pp. 209–228, Oct. 1973.
- [11] J. P. Webb, "Finite-element analysis of dispersion in waveguides with sharp metal edges," *IEEE Trans. Microwave Theory Tech.*, vol. 36, pp. 1819–1824, Dec. 1988.
- [12] B. Schiff, "Eigenvalues for ridged and other waveguides containing corners of angle  $3\pi/2$  or  $2\pi$  by the finite-element method," *IEEE Trans. Microwave Theory Tech.*, vol. 39, pp. 1034–1039, June 1991.
- [13] Z. Yosibash and B. Schiff, "Superelements for the finite element solution of two-dimensional elliptic problems with boundary singularities," *Finite Elements Anal. Des.*, vol. 26, pp. 315–335, Aug. 1997.
- [14] G. Strang and G. J. Fix, *An Analysis of the Finite Element Method*. Englewood Cliffs, NJ: Prentice-Hall Inc., 1973.
- [15] L. Fox, P. Henrici, and C. Moler, "Approximations and bounds for eigenvalues of elliptic operators," *SIAM J. Numer. Anal.*, vol. 4, pp. 89–102, Mar. 1967.
- [16] B. Schiff and Z. Yosibash, "Eigenvalues for the Laplacian over domains containing re-entrant corners by the finite element method," unpublished.
- [17] H. H. Meinke, K. P. Lange, and J. F. Ruger, "TE and TM waves in waveguides of very general cross section," *Proc. IEEE*, vol. 51, pp. 1436–1443, Nov. 1963.
- [18] A. F. Peterson, *Computational Methods in Electromagnetism*. Piscataway, NJ: IEEE Press, 1998.
- [19] Z. Pantic-Tanner, J. S. Savage, D. R. Tanner, and A. F. Peterson, "Two-dimensional singular vector elements for finite-element analysis," *IEEE Trans. Microwave Theory Tech.*, vol. 46, pp. 178–184, Feb. 1998.
- [20] J. Gil and J. Webb, "A new edge element for the modeling of field singularities in transmission lines and waveguides," *IEEE Trans. Microwave Theory Tech.*, vol. 45, pp. 2125–2130, Dec. 1997.

**Bernard Schiff** received the B.Sc. and Ph.D. degrees from Imperial College in London, London, U.K., in 1952 and 1955, respectively.

After a short period in industry, in 1958 he joined the Applied Mathematics Department, Weizmann Institute of Science, Rehovot, Israel. From 1966 to 1999, he was with the School of Mathematics, Tel Aviv University, Tel Aviv, Israel, where he was appointed Senior Lecturer and later Associate Professor in applied mathematics. His initial research was in computations for quantum mechanics, firstly in solid-state physics and later in the determination of energy levels for "two-electron atoms" to an accuracy high enough to include contributions from relativistic effects. From 1974 to 1975, he spent a sabbatical leave at Brunel University, Uxbridge, U.K., where he was introduced to the finite-element method, and was then involved with applying it to solve elliptic problems over domains with singularities on the boundary. Since then, his main research interest had been in this field. The methods developed have been applied mainly to problems in fracture mechanics, but the techniques have also been adapted to determine cutoff frequencies for waveguides whose cross section contains re-entrant corners. He passed away in 1999.



**Zohar Yosibash** received the B.Sc. degree in aeronautical engineering from the Israel Institute of Technology—Technion, Haifa, Israel, in 1987, the M.Sc. degree in applied mathematics from Tel Aviv University, Tel Aviv, Israel, in 1992, and the D.Sc. degree in mechanical engineering from Washington University, St. Louis, MO, in 1994.

He is a Senior Lecturer and the Head of the Computational Mechanics Laboratory, Mechanical Engineering Department, Ben-Gurion University of the Negev, Beer-Sheva, Israel. He served as an Engineering Officer in the Israel Air Force (1987–1992), and as a Visiting Assistant Professor in the System Science and Mathematics and Mechanical Engineering Departments of Washington University, from 1994 to 1995. In 1995, he joined Ben-Gurion University of the Negev as a Lecturer and, since 1997, he has been a Senior Lecturer. His research interests include singular solutions of elliptic boundary value problems (especially generalized fracture mechanics), theoretical and applicative aspects of the p-version of the finite-element method applied to linear and nonlinear problems in solid mechanics, and adaptivity.